NREL/CP-510-22920 • UC Category: 1250

Performance of Single-Junction a-Si Modules under Varying Conditions in the Field

J.A. del Cueto and T.J. McMahon

Presented at the 26th IEEE Photovoltaic Specialists Conference, September 29–October 3, 1997, Anaheim, California

National Renewable Energy Laboratory
1617 Cole Boulevard
Golden, Colorado 80401-3393
A national laboratory of
the U.S. Department of Energy
Managed by Midwest Research Institute
for the U.S. Department of Energy
under contract No. DE-AC36-83CH10093

Prepared under Task No. PV706101

September 1997

PERFORMANCE OF SINGLE-JUNCTION A-SI MODULES UNDER VARYING CONDITIONS IN THE FIELD

J.A. del Cueto and T.J. McMahon
National Renewable Energy Laboratory, 1617 Cole Blvd., Golden, CO 80401

ABSTRACT

We report on the actual performance of large-area photovoltaic (PV) modules deployed outdoors, which are representative of single-junction amorphous silicon (a-Si) thin-film technology. They are part of the performance and energy-ratings testbed (PERT) at the Outdoor Test Facility (OTF) and are under continuous measurement and load conditions, as executed by a data acquisition system (DAS). The goals are to analyze and compare energy production and performance for various PV technologies deployed in actual field conditions and to validate the PV energy-ratings methodology being developed for modules. For single-junction a-Si, we found the effective efficiency is very similar to that measured at standard conditions.

INTRODUCTION

The current system of appraising PV module energy production capacity and performance in the field, via measurements of current-voltage (I-V) characteristics performed at standard reporting conditions (SRC, 1000 W/m^2 and 25°C), lacks accuracy for some technologies. Because of conditions encountered in the field, such as varying temperatures and illumination levels substantially different from those at SRC, such assessment can be difficult and imprecise. A methodology for rating PV modules is being developed at NREL, as a tool to assess energy production capacities of diverse PV technologies.

The PERT system and modules deployed at the OTF function to perform the experimental measurements and performance validation of the energy-ratings methodology for diverse PV technologies (c-Si, p-Si, a-Si, CIS, CdTe). Currently, the system holds 15 modules. An expansion is under way so that by mid 1998, an additional 30 modules will be deployed. Modules deployed on the PERT system have their I-V curves taken by the data acquisition system (DAS), along with irradiance and temperature. The DAS is a commercially available unit, a RAYDEC RD-1200 Multi-Tracer II. During the course of a year, each module typically accrues 6000 records (IV curves).

Our analysis focuses on the performance of two, large-area (1.1544 m^2 aperture area), single-junction, a-Si thin-film PV modules, comprised of 66 cells apiece connected in series, and monolithically integrated and encapsulated with a glass-to-glass seal. Our choice of analysis of this technology is based on the simplicity of this system which employs representative design components and strategies extant in other PV technologies. With this choice, we hope to gain insight into PV performance in the field before proceeding to analyze more complex technologies.

EXPERIMENTAL

Modules on the PERT system are assembled facing due south ±2° and at a fixed tilt of 40°±1°, which corresponds to the approximate latitude for the OTF site, 39.74° N. The two a-Si modules reported on, serial numbers 51-13 and 47-37, were put outdoors on June 13, 1996. Prior to deployment, these modules received certified, NREL baseline IV measurements. For one module, shunt resistance measurements of each cell were performed using a technique developed by one of the authors [1].

Global solar irradiance was measured with a pyranometer that is mounted on the same structure and in close proximity to the modules, at the same plane-of-array (POA) tilt. Thermocouples are fixed to the backs of each module. During hours of daylight and once every 30 minutes, the DAS performs measurements of the IV characteristics of each module via programmable load and fixed shunt resistors. Each module is connected to the DAS using four electrical leads - two for carrying the current and two for making voltage measurements as close to the module as practical. This measurement scheme traces out the electrical characteristics of each module in 10 seconds or less, from about 50 millivolts above the short-circuit current (Isc) point up to the open-circuit voltage (Voc). Along with IV data, measurements of POA irradiance and temperature of the module are performed by the DAS and saved as one record by the PC onto electronic media.

Using spreadsheet software, each record was reduced to fundamental IV parameters. The precise value of Isc for each record was determined by linear regression of IV data using points near Isc, where the voltage is typcially 10% or less of Voc. This analysis also yields the slope at

Isc (effective Rsc), and statistical parameters such as the variance, standard deviation, and probable error. The precise value for Voc is also determined by similar linear regression using IV data which exhibit current values 12% or less of Isc. This analysis also yields the slope at Voc (effective Roc) and the variance, standard deviation, and probable error. The maximum power is calculated from the maximum product of current times voltage; the fill factor is calculated by dividing maximum power by the product of Isc times Voc. The aperture-area efficiency is derived by division of maximum power by the product of aperture-area times measured irradiance for that record. The reduced IV parameters plus irradiance, date, time, and module temperature are saved on the spreadsheet and accumulated for all records of both a-Si modules.

Prior to final analysis, the data for the two a-Si modules were filtered to minimize errors that might arise from variations in irradiance between the time of measurement of the IV characteristics and that of the measurement of the irradiance; such conditions may be encountered when making measurements during the passage of clouds. Filtering was performed by linear regression of all short-circuit current against irradiance levels for all records of each module. The final data set arrived at was chosen at the 95% confidence level about this regression and consists of about 7000 records for each module. This set and/or subsets of this set, were subsequently analyzed for variations versus time, temperature coefficients of IV parameters as functions of irradiance, and overall effective module power-energy output and efficiency.

RESULTS ANALYSIS AND DISCUSSION

The aperture-area efficiency and fill factor values of module no. 47-37 are plotted against time in Fig. 1 and are read from left and right vertical axes, respectively. These data include all possible module temperatures, but only those data for which the irradiance values lie in a narrow band of 1000 ± 50 W/m^2. This figure exposes the initial degradation of the module's efficiency from 5.4%-5.8% down to 4.6% within 4 months of exposure. During the same time, the fill factor is shown to degrade from about 63%, down to about 55%. Similar trends are exhibited for the second module, no. 51-13, with noted exceptions: during the first week, the initial drops in both the efficiency and fill factors are larger; afterwards, the efficiency and fill factor are offset to lower values by 5 and 6-7 relative percent, respectively. Prior to deployment, baseline, outdoor IV measurements performed near SRC resulted in aperture-area efficiency of 6.4% for both modules. Module temperatures for data in this figure lie in the range 10°-75°C, with the bulk of the data occurring between 40°-70°C. The efficiency data shown in Fig. 1 are not corrected for temperature. However, these corrections are small, less than or equal to 5 relative percent maximum spread for all temperatures.

Fig. 1, shows that the source of degradation correlates well with changes occurring in the fill factor. Fig. 2 reveals the nature of the change in fill factor more clearly. It depicts the calculated slope at open-circuit (Roc) and short circuit (Rsc) conditions plotted against time, and is read from left and right vertical axes, respectively, for module no. 47-37. The data set plotted on Fig. 2 is a subset of that plotted on Fig. 1, which includes only those data with substantial numerical significance and accuracy.

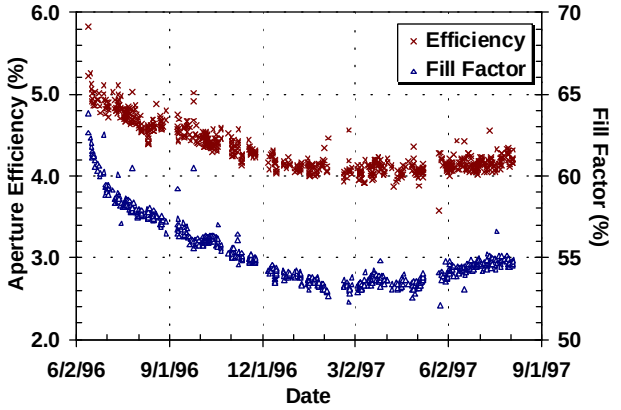

Figure 1. Module 47-37. Efficiency (x) and fill factor (Δ) plotted against time, for irradiances: 1000 W/m^2 ± 5%.

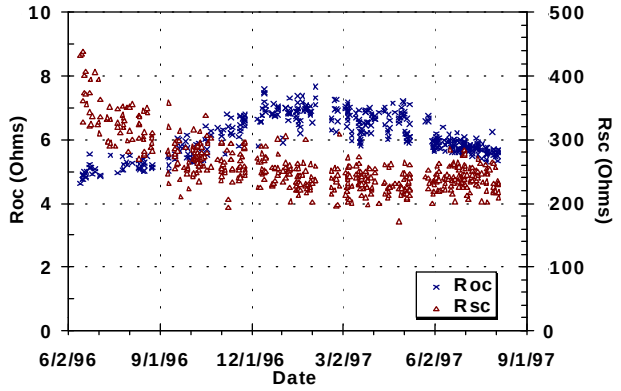

Figure 2. Module 47-37. Slope at open-circuit, Roc (x) and short-circuit, Rsc (Δ), plotted against time, for irradiances: 1000 W/m^2 ± 5%.

Fig. 2 shows that the initial degradation in fill factor is correlated with a drop in Rsc, from about 400 ohms to 250 ohms in the first 4 months of exposure, although the drop in Rsc does not seem be the direct cause. Thereafter, Rsc shows insignificant change. Conversely, modifications in fill factor, starting from about 4 months after deployment, appear associated with changes occurring in Roc, which rises from about 5.5 ohms up to 7 ohms, and then drops down to 5.5 ohms after about 13 months of deployment. Very comparable trends are exhibited by the second a-Si module, no. 51-13, with the modulus of Rsc displaced to values 70-80 ohms lower and that of Roc displaced to values 1 ohm higher, than those of module no. 47-37.

For the analysis of the temperature coefficients of IV curve parameters (Voc, Isc, etc.), we chose to exclude the initial 4 months of data, estimated to represent an exposure of 680 hours at 1-sun. Also excluded were those data in which module temperatures were not available. Figs. 3, 4, 5, and 6 depict the results of this analysis, for module no. 47-37, which, respectively, show module Voc, fill factor (FF), efficiency, and Isc, their average values plus their values referenced to 25°C temperature, along with temperature coefficients thereof plotted in intervals of irradiance levels from 25 to 1200 W/m^2.

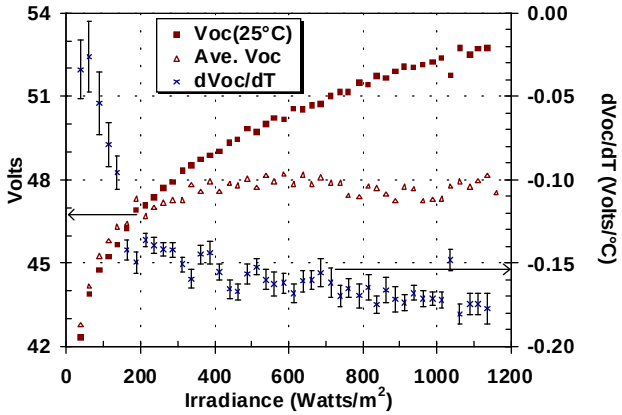

Figure 3. Module 47-37. Voc at 25 °C (■), average Voc (Δ), and temperature coefficients dVoc/dT (x) plotted vs. irradiance.dVoc/dT error bars depict ± 1 std. deviation (σ).

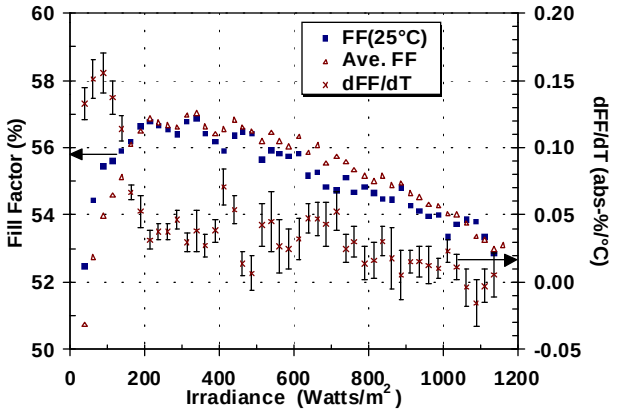

Figure 4. Module 47-37. Fill factor, FF, at 25 °C (■), average FF (Δ), and temperature coefficients dFF/dT (x) plotted vs. irradiance. dFF/dT error bars depict ± 1 σ.

Fig. 3 reveals that module Voc, referenced to 25°C, rises quickly at low irradiance, followed by a lower rate of rise at high irradiance. The temperature coefficient of Voc is negative for all irradiance levels, but its modulus rises from a very low value to larger values with increasing irradiance. In Fig. 3, the fact that average Voc in each interval saturates at 48 volts at higher irradiance (>400 W/m^2) is a result of the effects of the negative temperature coefficients convoluted with correspondingly increasing module temperatures at those higher levels.

Fig. 4 indicates that the module fill factor has rather small temperature coefficient above 200 W/m^2 irradiance. It shows the module fill factor increasing rapidly at low irradiance levels, reaching a maximum value between 200 - 400 W/m^2 , and then slowly decreasing at higher levels. These data are consistent with shunting paths limiting the fill factor at low irradiance levels and series resistance at the higher levels, as per reference [1].

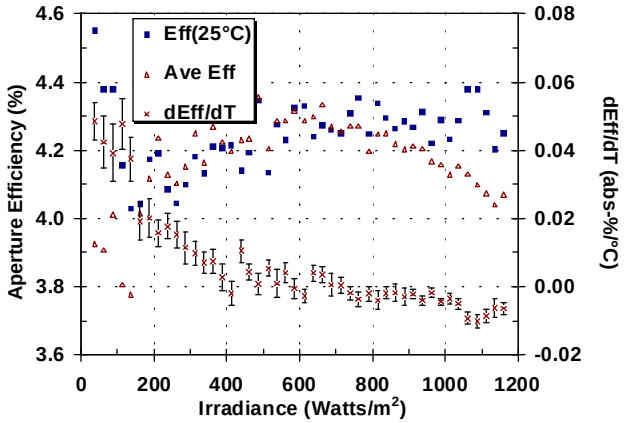

Figure 5. Module 47-37. Efficiency at 25 °C (■), average efficiency (Δ), and temperature coefficients dEff/dT (x) plotted vs. irradiance. dEff/dT error bars depict ± 1 σ.

The data plotted in Fig. 5 show the efficiency to have an insignificant temperature coefficient above irradiance levels of 300 W/m^2, with somewhat higher temperature dependence at lower light levels. The differences in efficiency data between the average and reference temperature (25°C) values are generally within 1-2 standard deviations of each other. The data in Fig. 5 do not support the notion that at low light levels the efficiency falls off; instead the data appear to suggest that the efficiency is not significantly affected by irradiance level.

Because average module temperature increases with higher irradiance, the same analysis was carried out including only those data exhibiting temperatures in the range of 20°-40°C. Although the results of this analysis exhibit more dispersion, the basic inferences and conclusions are identical to those garnered from the less restrictive data presented in Figs. 3-6. Module efficiency appears insignificantly affected by irradiance levels.

Fig. 6 depicts Isc normalized to one 1-kW irradiance, and its temperature coefficient normalized to average Isc plotted versus irradiance. This graph shows how it is possible for both Voc and FF to drop off at low irradiance values, while the efficiency remains relatively unchanged. Normalized Isc appears constant above 200 W/m^2, whereas at lower values, it increases by 20%-30%. The fact that Isc normalized to irradiance exhibits an increase at low irradiance values remains unexplained. Considering the larger sun angles associated with illumination at these levels, one would expect a drop in Isc per unit value of irradiance, which is contrary to the data. This increase

occurs even after accounting for a probable 4%-5% change in the calibration of the pyranometer due to illumination at the low incidence angles.

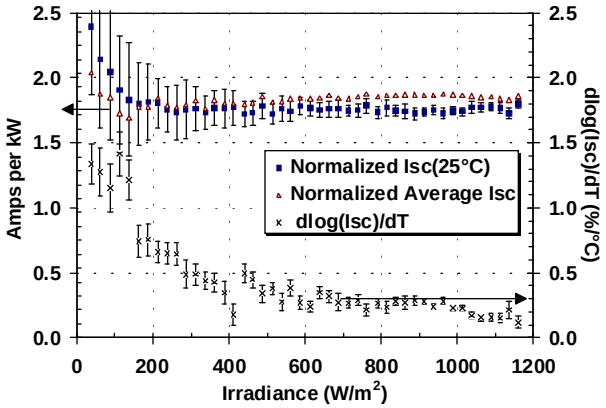

Figure 6. Irradiance-normalized Isc at 25°C(■) and average Isc (Δ), and temperature coefficients(x) vs. irradiance, for Module 47-37. Error bars depict ± 1 standard deviation.

Toward the goal of achieving practical energy ratings, we have analyzed average, daily, module power output and irradiance, rationed by month. For this analysis, average module power and irradiance were calculated and plotted against time-of-day. These data were integrated over time, arriving at average daily module energy production and insolation for each month. Dividing the average module energy production by the insolation yields the effective efficiency. These data are shown graphically in Fig. 7, the effective aperture-efficiency plotted by month. It is evident this effective module efficiency differs little from that shown in Fig. 1.

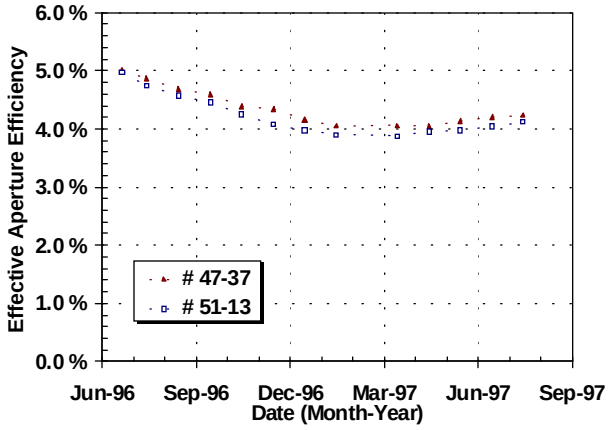

Figure 7. Effective average aperture-area-based efficiency for both modules, 51-13 and 47-37, plotted by month.

Parameters from dark I-V curves and cell shunt resistance values were introduced into an application software (PSpice) circuit model of this series-connected module. The drop in FF at 50 W/m^2 is easily accounted for by a distribution of cell shunt resistances varying between 5 and 80 ohms. A calculated drop in peak efficiency of 40% from the value at 1000 W/m^2 is found for the assumption of a constant normalized Isc with irradiance. However, the normalized Isc has a 20%-30% increase in irradiance below 150 W/m^2, which nearly eliminates any change in peak efficiency. Furthermore, the continued rise in efficiency in the 200-1000 W/m^2 that one would expect from calculation does not occur, due to series resistance effects that can also be calculated [1]. Combining all these effects results in efficiency which is a fairly weak function of irradiance and temperature.

Because the module shunt resistance is 3.2 kohms (i.e. the sum of the cell shunts) and Rsc has a slope of 230 ohms at 1000 W/m^2, Rsc is determined by voltage-dependent carrier collection. As pointed out, variations in this slope are not large enough to be the direct cause of the change in efficiencies noted in Fig. 1. However, at 1000 W/cm^2 Roc has a 7 ohm slope: 5 ohms are due to series resistance and 2 ohms are due to diode factor and saturation current. Because series resistance is not expected to change, seasonal change in diode factor (A) and saturation current must be enough to account for the seasonal change in FF by its effect on Roc (A changes from 1.75 to 2.25 with light soaking [2]).

CONCLUSIONS

The effective module efficiency derived from energy-out divided by energy-in calculations, for all field conditions, shows little variance from that which is measured at near-SRC conditions. This is due to the unchanging nature of the efficiency with illumination level and temperature. This implies that energy-rating single-junction a-Si technology may be had via convolution of the efficiency at SRC with illumination level, provided one knows the light-soaked, seasonal value of efficiency. The seasonal variations in the efficiency appear well-correlated to seasonal changes in the slope of the IV curve at open-circuit conditions, which likely arise from changes in diode factor.

ACKNOWLEDGMENTS

This work was performed under U.S. Department of Energy contract number DE-AC36-83CH10093.

REFERENCES

1. McMahon, T.J., T.S. Basso, and S.R. Rummel, "Cell shunt resistance and photovoltaic module performance," *25th IEEE PVSC proc.*,(1996) p.1291.

2. McMahon, T.J., J.P. Xi, "Light induced chance in a-Si:H material and p-i-n devices," *J. Non-Crystalline Solids* **77**, (1985) p.409.